

# Surface-Enhanced Raman Spectroscopy (SERS) for characterization SARS-CoV-2

Javier C. Ramirez Perez (✉ [jramire7@kent.edu](mailto:jramire7@kent.edu))

University of Sao Paulo

Daniele Durigon

University of Sao Paulo

---

## Research Article

**Keywords:** SARS-CoV-2, Virus, Surface-enhanced Raman spectroscopy, SERS, Silver Nanoparticles, Detection

**Posted Date:** March 30th, 2022

**DOI:** <https://doi.org/10.21203/rs.3.rs-1455994/v1>

**License:** © ⓘ This work is licensed under a Creative Commons Attribution 4.0 International License.

[Read Full License](#)

---

# Abstract

**Background:** The current coronavirus disease 2019 (COVID-19) pandemic caused by SARSCoV-2 standard assay relies on RNA purification, one-step retrotranscription, and quantitative PCR to identify SARS-CoV-2 (RT-qPCR). However, this standard procedure usually takes 4.0 h, particularly for the RNA extraction step. The goal of this study was to evaluate the performance of SERS using AgNPs, a simple and cost-effective method for quickly characterizing SARS-CoV-2. The study focused on the urgent need for high-performance screening, eliminating the time-consuming RNA extraction phase and reducing the time to virus characterization.

**Results:** AgNPs-SARS-CoV-2 samples prepared with inactivated SARS-CoV-2 produced SERS signals that were more than 105 times stronger than normal Raman (NR) spectra. According to the SERS spectra of the SARS-CoV-2 fingerprint, nucleic acids and aromatic amino acid side chains of these biomolecules may be adsorbed on the AgNPs surface's dense hot spots. With a virus detection limit of fewer than 103 vp/mL and RSDs of 20%, the SERS band intensities varied with the concentration of SARS-CoV-2.

**Conclusions:** A novel, simple, fast, cost-effective, and accurate protocol for acquiring strong, sharp, and reproducible SERS signal intensities of the SARS-CoV-2 virus has been developed. The SERS spectra collected exhibited SARS-CoV-2 virus detection limit, consistency, sensitivity, selectivity, and reproducibility. In the SERS spectra of SARS-CoV-2, the main vibrational acute and intense signal was identified in the 500-1700  $\text{cm}^{-1}$  range at 1007, 1221, 1270, and 1453  $\text{cm}^{-1}$ . These bands were identified in SARS-key CoV-2's structural proteins and nucleic acids, and were attributed to ubiquitous biomolecules. Our prospective contribution is aimed at combating the COVID-19 infectious disease in order to improve SARS-CoV-2 virus detection and characterization.

## 1. Introduction

Coronaviruses are named from the outer fringe, crown, or "corona" of embedded envelope protein that they have (Graphical abstract). Members of the Coronaviridae family are responsible for a wide range of animal and human diseases. Since 2003, coronaviruses began to attract broad interest with the zoonotic SARS-CoV. Following that, the appearance of MERS-CoV in 2012 confirmed coronaviruses as major causes of severe respiratory disease [1–3]. The severe acute syndrome coronavirus 2 (SARS-CoV-2) causes the current coronavirus infection disease-2019 (COVID-19) pneumonia, which has spread worldwide and poses a serious health hazard to humans. Until October 2020, it has been reported 44.88M confirmed cases and 1.178M deaths globally (WHO, 220/10/30), and these numbers are still growing [4]. SARS-CoV-2 is transmitted through respiratory droplets [5–7] and aerosols via person-to-person contact [8, 9]. The development of improved diagnostics is the major means of preventing the spread of the SARS-CoV-2 virus in the absence of a vaccine or generally effective and relevant treatments. Alternative detection, identification, and diagnostic procedures that can work alone or in conjunction with existing methods are still a priority. Currently, the methods for SARS-CoV-2 detection include electron microscopy (EM), real-time reverse transcription quantitative polymerase chain reaction (RT-qPCR) and serological

enzyme-linked immune-sorbent assay (ELISA) [7, 9]. However, EM is used only with limit detection around 10<sup>5</sup> particles per millilitre [10], RT-qPCR targeted viral specific RNA fragment with specific primers for the open reading frame 1ab (ORF1ab), nucleocapsid protein (N), envelope protein, membrane protein, or RNA-dependent RNA polymerase (RdRp) [5–9]. For RT-qPCR, RNA extraction from swab samples is required, which necessitates time-consuming pre-treatment that can take up to 4 hours, posing a hurdle to SARS-CoV-2 diagnosis [8–10]. Furthermore, ELISA is a widely utilized enzyme immunoassay for detecting a receptor utilizing antigen-specific antibodies that target immunological markers such as IgM and IgG antibodies [7, 8, 10]. Nonetheless, for the diagnosis of SARS-CoV-2 in human and environmental samples that lack immunological markers, this technique is still time-consuming and ineffective

[9, 10]. Raman spectroscopy is a vibrational spectroscopy of ability to detect chemical bonds via photon scattering, although the generated signals are extremely weak in comparison to the incident beam [10, 11]. SERS is a contemporary spectroscopic technique in which the Raman signal of a Raman-active molecule's functional group is considerably amplified when the molecule is adsorbed on the surface of specially prepared coinage metals, such as Ag, Au, or Cu. [11, 12]. The SERS amplification is caused by two separate phenomena: first, the traditional near-field electromagnetic effect, and second, the chemical effect [13], which allows for the detection of biomolecules' local composition at extremely low concentrations (down to a single molecule) [13, 14]. Furthermore, when the energy of an electronic transition is equivalent to the excitation source, the SERS approach delivers an amplification of several orders of magnitude. Signal enhancements as high as 10<sup>14</sup> times over normal Raman scattering have been reported [14]. Hence, a rapid, simple, accurate and reproducible method for characterization and detection of SARS-CoV-2 is extremely required in order prevent and to tackle the spread of this deadly disease. SARS-CoV-2 is an enveloped virus with a positive sense, single-stranded RNA genome. The corona viral genome encodes four major structural proteins, a large nucleocapsid (N) protein and three transmembrane proteins are incorporated into the viral lipid envelope: the spike (S), membrane (M) and the envelope (E), all of which are required to produce a structurally complete viral particle, individually, each protein primarily plays in the structure of the virus particle, but they are also evolved in other aspects of the replication cycle [15]. S trimers of SARS-CoV-2 bind to its receptor on the surface of target cells-angiotensin-converting enzyme 2 (ACE2) and mediate subsequent viral uptake and fusion. In doing so, S undergoes a substantial structural rearrangement from the prefusion form to the postfusion form. The overall architectures of both forms are highly conserved among coronaviruses [16]. A few studies have been reported in the literature, for example, Turnip Mosaic virus (TuMV) coat protein prepared using silver colloid solution, the SERS bands recorded in the region (300–1700 cm<sup>-1</sup>) assigned nucleic acids and amino acids [17]. SERS was used to identify seven food- and waterborne viruses, including norovirus, adenovirus, parvovirus, rotavirus, coronavirus, paramyxovirus, and herpesvirus. After drying, the samples were deposited onto silicon wafers coated with AuNPs (Klarite™), and traditional biomolecules of cells, such as nucleic acids, proteins, or amino acids, as well as other components of viruses, were analyzed. They were also able to distinguish between viruses with and without envelope using PCA. A viral detection limit of 10<sup>2</sup> vp/mL was also attained [18]. SERS signals were acquired using a silver nanorods

array functionalized with the cellular receptor angiotensin-converting enzyme 2 (ACE2), which were combined with multivariate analysis to diagnose SARS-CoV-2 in environmental specimens [7]. In this study, we presented the viability of employing SERS in combination with AgNPs substrates to detect SARS CoV-2 as a diagnostic approach that is rapid, non-invasive, and has good reproducibility and accuracy, as an alternative to existing biological tests.

## 2. Methods

### 2.1 Acquisition and processing samples

SARS-CoV-2 samples were collected from the department of Microbiology, Institute of Biomedical Sciences (IBS) at University of Sao Paulo, Brazil. Previously, NP swabs were collected in a tube containing a few millimeters of viral transport medium (VTM) from three patients with confirmed COVID-19 infection in August 2020, according to an IBC-approved methodology; all samples were SARS-COV-2 positive by RT-qPCR analysis. At the Nuclear and Energy Research Institute (IPEN), viral cells were inactivated by gamma irradiation ( $5 \times 10^6$  rad). A stock SARS-CoV-2 viral cells solution was set up at concentration of  $1 \times 10^5$  vp/mL for each sample and stored at  $-80$  °C. A total of 12 SARS-CoV-2 samples were analysed in the SERS experiment from August to September, 2020. Each SERS spectrum was averaged from 18 different spots from a single sample. Gamma radiation is an ionizing radiation that is often used to render high-risk group viruses dormant in maximum containment laboratories. It's also the best way to keep viral morphology and protein structures intact [20, 21]. A minimum dose of 1 Mrad (10 kGy) was recently reported to inactivate  $10^{6.5}$  TCID<sub>50</sub>/ml (tissue culture infectious dose) with negligible influence on subsequent polymerase chain reaction (PCR) assay in SARS-CoV-2 [21], but whether this claim is accurate for SARS-CoV-2 requires more investigation. The sample SARS-CoV-2-SERS-AgNP active substrate was prepared by 0.35  $\mu$ L drop of SARS-CoV-2 onto AgNPs substrate, the mixture ratio of the sample and AgNPs was 1:4, the diameter of the active substrate was approximately 2 mm. In this study we proposed an experimental procedure of SERS technique for identification, detection and diagnostic of SARS-CoV-2 (Fig. 1).

### 2.2 Limit of detection dilution sample preparation

The limit of detection (LOD) of SARS-CoV-2 was performed by sequentially diluted from  $10^5$  vp/mL SARS-CoV-2 sample concentrate viral cells particle stock solution to  $10^2$  vp/mL diluted in 1:10, 1:100 and 1:1000 ratios using ultrapure water (nuclease-free molecular biology grade (#20022103), Austin, TX-USA). Samples were further stored at  $-80$ °C, before SERS analysis in order to achieve a detection sensitivity of SARS-CoV-2.

### 2.3 Preparation of silver nanoparticles-SERS active substrates

Silver nanoparticles (AgNPs) were synthesized by reduction of silver nitrate ( $\text{AgNO}_3$ ) solution with sodium citrate based on the method reported by Lee and Meisel [22].

Briefly, In 500 mL distilled water, 90 mg of  $\text{AgNO}_3$  was dissolved. The solution was brought to a boil. The solution was then given a 10 mL aliquot of 1 percent sodium citrate and kept boiling until the volume was reduced to half of what it had been. The SAXS method is utilized to measure the average size of the nanoparticles (60 nm), and its complete structural characterization, including electron microscopy pictures, has previously been published [12, 35]. In the supplementary material (Figs. 1SA, 1SB) a small aliquot of AgNPs stock solution was diluted with distilled water, and the UV-Vis absorbance measurement revealed a characteristic peak of AgNPs at 390 nm. All of the samples were using the AgNPs that were synthesized.

## 2.4 Surface-Enhanced Raman Spectroscopy Measurements spectral acquisition

SERS measurements were acquired using a Renishaw inVia Reflex Raman Microscopy System Leica DM2500 M (Renishaw PIC., New Mills, Wotton-under-Edge Gloucestershire, UK) equipped with 500 mW maximum high power, diode laser emitted a 785 nm line which was used as an excitation source. The laser light was focused on a sample mounted on a tridimensional stage with a 50x objective lens (numerical aperture (NA) = 0.75) that concentrated the laser to a spot size of roughly 2.5  $\mu\text{m}$  after passing through a line filter. A 1040 x 256 pixels Peltier-cooled RenCam CCD array detector, which allowed registering the Stokes part of Raman spectra with 5–6  $\text{cm}^{-1}$  spectral resolution and 2  $\text{cm}^{-1}$  wavenumber accuracy, The Raman scattering signals were recorded using a 1200 line network of diffraction that was thermoelectrically cooled.. The instrument was calibrated using a silicon wafer with the band center at 520  $\text{cm}^{-1}$ . The Raman shift range has been set from 550 to 1700  $\text{cm}^{-1}$  (static mode) and 300 to 3500  $\text{cm}^{-1}$  (extended mode) (SynchroScan mode), because these areas have interesting SARS-CoV-2 bands. The exposure time was 10s, 10 accumulations, with the power of the laser set to 1% (equal to 5mW or less), (Fig. 1).

## 2.5. Data Processing

The OriginPro 2018.64 bit software was used to treat the NR and SERS spectra in this investigation. The AgNPs SERS active substrate was calibrated using pMBA typically standard SERS analyte, because it tends to adsorb efficiently on AgNPs surface [27]. The SERS active-substrate exhibits high sensitivity, an enhancement factor approximately  $4.4 \times 10^7$ , reproducibility (relative standard deviation, RSD = 4%) and stability of near 2 months of the recorded SERS spectra Figs. 3S and 4S (SM). Pre-processing of SERS spectra was done according to a procedure for spectroscopic methods to examine biological materials that was approved [36]. Briefly. Rubber band baseline correction subtracts a rubber band, which is stretched bottom up at each spectrum, eliminating slopes. Differentiation (Savitzki-Golay) (SG) method has the advantage of eliminating slopes while also resolving overlapped bands as well as smoothing, minimum noise fraction. Amide I/II normalization forces all spectra to have the same a Raman intensity at the amide I/II peak. units

# 3. Results

### 3.1. Features of SERS spectrum and Normal Raman of SARS-CoV-2

The SERS technique was employed for the characterization and detection of SARS CoV-2. The average of 12 SERS spectra of SARS-CoV-2-AgNP substrate samples acquired during the period from 08–14 to 09-23-2020 are shown in Fig. 2 in perspective. The SERS spectra of SARS-CoV-2 exhibits a number of marker modes spreading well all over the region between 1000 and 1700  $\text{cm}^{-1}$ . Except the obvious minor differences in intensities, orientations and peak sharpness in relative band width and intensity, the SERS spectra obtained over the period of testing were identical in the spectral region 500–1700  $\text{cm}^{-1}$ . The SERS spectra have a high sensitivity, a signal amplification of up to  $7.0 \times 10^5$ , and are reproducible across the period of time testing. Large enhancement factors of the electromagnetic field are only accomplished in very tiny areas of the surface of nanostructured metals, due to the increased degree of AgNP aggregation, which is critical for forming efficient "hot spots." [14, 19]. Because of the high density of the hot spots, only a tiny percentage of SARS-CoV-2 biomolecules adsorbed on junctions of two or more AgNPs resulted in a greatly increased and reproducible SERS signal [23]. SARS-CoV-2 with and without spike AgNPs was firstly tested as a proof-of-concept demonstration of the protocol developed in this study. Figure 3Aa show the representative Normal Raman (NR) spectra tests in the range of 500 to 1700  $\text{cm}^{-1}$  and and Fig. 3Ba in the spectral region of 300–3500  $\text{cm}^{-1}$ . The recorded NR spectra were highly reproducible, and reveal no signal besides a weak band with maximum c.a. 1400  $\text{cm}^{-1}$  comparing to the incident beam. The Raman intensity in the NR spectra without AgNPs varies between 2 and  $5 \times 10^2$ . Correspondingly, the NR spectrum of clean  $\text{CaF}_2$  glass slide used as platform to spot the SARS-CoV-2 sample (Fig. 3Ab and Fig. 3Bb) exhibits no signal, possibly as a result of the SARS-CoV-2 viral suspension sample's transparency,  $\text{CaF}_2$  was utilized as the window material in order to eliminate multiple internal reflections. In contrast, the SERS spectra of SARSCoV-2 measurements in the spectral region between 1000 and 1700  $\text{cm}^{-1}$  indicate pronounced band enhancement, especially the SERS signals centered around 1000  $\text{cm}^{-1}$  (Figs. 3Ac and 3Bc), which shows highly reproducible bands with great uniformity and extraordinary sensitivity. The orientation on the surface of aggregated AgNPs could also explain the adsorption of several amino acids with cyclic R side chains, such as aromatic ring in phenylamine at 1007  $\text{cm}^{-1}$ . As can be shown, our SERS-active substrate achieves a substrate with a very high enhancement magnitude, ranging from 0.2 to  $1.6 \times 10^6$  (Raman Intensity). However, some bands in the SERS spectra of SARSCoV-2 show fluctuation in relative band shapes and intensities in other spectral regions between 400 and 1000  $\text{cm}^{-1}$  and 1500 to 3500  $\text{cm}^{-1}$ , respectively. This is attributable to the fact that the SARS-CoV-2 biomolecules' adsorption behavior on AgNPs aggregates. The enhancement of the electromagnetic field in the slits between AgNPs aggregates has been reported to be much higher [19, 23]. Thus, before SERS measurements AgNPs are usually aggregated/agglomerated to generate such slits. Low-intensity shape bands were found, as well as a lack of high signal-to-noise ratios, implying the presence of several overlapping peaks. This could be because SARS-CoV-2 includes numerous biomolecules that all co-adsorb on the surface of AgNPs, causing peak broadening. Furthermore, the orientation of the adsorbate on the hot spots generated between the intraparticle gaps of AgNPs is likely modulated by the relative low intensity of the molecular components. In section 3.4, the SERS spectra,

band intensities, and marker modes recorded in the 500–1700 and 300–3500  $\text{cm}^{-1}$  regions, respectively, are examined in better detail.

### 3.2. SERS reproducibility of SARS-CoV-2

A total of 9 SARS-CoV-2 SERS spectra were acquired from 3 random places on the same active substrate for varied concentrations to demonstrate the reproducibility of SARS-CoV-2 SERS spectra. The experiment was conducted by dilutions of inactivated SARS-CoV-2 (stock solution) from  $10^5$  vp/mL to  $10^4$ ,  $10^3$  and  $10^2$  (vp/mL) using ultrapure water, which served reference (Fig. 4A-D). Except for small intensity fluctuations in some bands, the SERS spectra varied with SARS-CoV-2 concentration, and the majority of the bands showed highly enhanced and reproducible SERS signals, implying the efficacy of AgNPs aggregate substrates. The excellent reproducibility could be ascribed to the virus cells' high density distribution, which indicates that most of the macromolecules of SARS-CoV-2 come into direct contact with the AgNPs' hot spots, which possible benefit to obtain a uniform SERS signal. We observed significant SERS signal enhancement with the concentration of SARS-CoV-2. For instance, high signal enhancement *ca.*  $6.5 \times 10^5$  times over NR scattering is achieved for  $10^5$  vp/mL of SARS-CoV-2 (Fig. 4A). In the SERS spectra, we identified the most significant bands as well as their reproducibilities reported as relative standard deviations (RSDs) at:  $1007 \text{ cm}^{-1}$  (4%);  $1144 \text{ cm}^{-1}$  (15%); and  $1270 \text{ cm}^{-1}$  (22%). The signal enhancement declined to *ca.*  $3.5 \times 10^5$ ,  $1 \times 10^5$  and  $4.3 \times 10^4$  for SARS-CoV-2 concentrations of  $10^4$ ,  $10^3$  and  $10^2$  vp/mL, respectively, for each intensity, including RSDs at:  $1007 \text{ cm}^{-1}$ ,  $1144 \text{ cm}^{-1}$ , and  $1270 \text{ cm}^{-1}$  detected for each intensity  $1007 \text{ cm}^{-1}$ ,  $1144 \text{ cm}^{-1}$ , and  $1270 \text{ cm}^{-1}$  (Fig. 4B-D).

For SERS quantitative research, less than 20% variance in SERS intensity between different locations of the active substrate is acceptable [25], in agreement with our findings. In addition, the SERS spectra for  $10^5$  vp/mL SARS-CoV-2 concentration were recorded by mapping a small area ( $20 \mu\text{m} \times 20 \mu\text{m}$ ) on the slide in the range of 500 to  $1700 \text{ cm}^{-1}$  (Supporting material Fig. 4S). The high reproducibility in this investigation can be ascribed to a homogeneous mixing of SARS-CoV-2 viral suspension and AgNPs of the same size (60 nm) and shape (spherical).

### 3.3 Limit of detection (LOD) of SARS-CoV-2 based on SERS method

The LOD was explored by comparing SERS signal enhancement with SARS-CoV-2 concentration; for instance, for  $10^5$  vp/mL high signal enhancement of *ca.*  $6.5 \times 10^5$  times over NR scattering was achieved (Fig. 5A). The signal enhancement declined to *ca.*  $3.5 \times 10^5$ ,  $1 \times 10^5$  and  $4.3 \times 10^4$  for SARS-CoV-2 concentrations of  $10^4$ ,  $10^3$  and  $10^2$  vp/mL, respectively (Fig. 5B). The LOD was defined in the literature as the concentration of SARS-CoV-2 for which the strongest signal of SERS enhancement was equal to 3 times the background SERS signal intensity, with the background SERS signal intensity referring to the SERS signal from a sample with virus cells concentration of 0 [26]. In order to determine the LOD, the SERS intensities of three peaks at  $1007$ ,  $1144$ , and  $1270 \text{ cm}^{-1}$  were notably strong and the intensity of the peaks increased when the viral cell concentration of SARS-CoV-2 increased. The peak at  $1007 \text{ cm}^{-1}$ ,

on the other hand, was one of the strongest for SARS-CoV-2, and its intensity increased as the concentration of SARS-CoV-2 increased. As a result, the peak at  $1007\text{ cm}^{-1}$  was chosen as a hint vibration to estimate SARS-CoV-2 concentration and to evaluate the LOD for SARS-CoV-2 samples. The peak intensity at  $1007\text{ cm}^{-1}$  ( $I_{1007}$ ) was plotted as a function SARS-CoV-2 concentration (Fig. 5C). The lowest concentration of SARS-CoV-2 found by this approach was lower than  $10^3\text{ vp/mL}$ , based on the average and 3 times of the SERS signal marked as control. The peak intensity ( $I_{1007}$ ) against the concentration of SARS-CoV-2 (vp/mL) with an  $R^2$  value of 0.96 confirming that the lowest concentration of SARS-CoV-2 detected with this assay may be around  $10^3\text{ vp/mL}$ .

### 3.4. SERS characterization of SARS-CoV-2

The current investigation, which took place from August to October 2020. The SERS technique was used to explore using AgNPs, SARS-CoV-2 characterisation and detection of key biomolecules such as structural proteins derived from SARS-CoV-2 composition. The average typical SERS spectra of SARS-CoV-2 mixed with aggregated AgNPs are shown in the region between  $500$  and  $1700\text{ cm}^{-1}$  (Fig. 6A) and  $300$  and  $3500\text{ cm}^{-1}$  (Fig. 6B), respectively. Table 1 shows the complete list of peaks wavenumber for SARS-CoV-2 as well as suitable tentative biomolecules assignments. The primary vibrational sharp and intense signals are visible in the SERS spectrum of SARS-CoV-2 at  $1007$ ,  $1221$ ,  $1453$  and  $1270\text{ cm}^{-1}$ ; in the mid intense at  $1095$ ,  $1144$ ,  $1580\text{ cm}^{-1}$ ; broad low intense at  $1500$  and  $733\text{ cm}^{-1}$ ; low intense at  $1405$ ,  $954$ ,  $1381$ ,  $1304\text{ cm}^{-1}$ ; and very low intense signals in the region between  $500$  and  $887\text{ cm}^{-1}$ . The pronounced intense band centred at  $1007\text{ cm}^{-1}$ , which is assigned to Phe marker, and the C-C skeletal stretching vibration of the phenylalanine ring combined with C-H in plane. Other vibrational modes of Phe located at  $1001\text{ cm}^{-1}$  attributed to the symmetric ring breathing mode;  $1018$  and  $1022\text{ cm}^{-1}$  assigned to the in-plane C-H bending, at  $1032\text{ cm}^{-1}$  attributed to in-phase motion  $\nu(\text{C-C})$  and  $\delta(\text{C-C-H})$  [12]. The next intense band at  $1221\text{ cm}^{-1}$  is ascribed to  $\text{PO}_2^-$ ,  $\text{NH}_2$  markers of amide III, which result from the coupling of  $\nu(\text{C-N})$  and  $\delta(\text{N-H})$ , although it has a weak band in the region  $300\text{--}3500\text{ cm}^{-1}$ , it is discernible (Fig. 6B) and has a low signal-to-noise ratio suggesting the presence of overlapping peaks. This is because SARS-CoV-2 cells contain numerous macromolecules that likely co-adsorb on AgNPs surfaces, resulting in peak reduction and distortion. Strong bands at  $1070\text{ cm}^{-1}$  attributed to  $(\gamma\text{-C-N})$  also identified in the SERS spectra of other viruses [17, 18]. Vibrational modes exist in the amide I, II and III, which are conformational sensitive. Primary C=O stretching, in-plane modes of N-H bending, and  $\nu(\text{C-C})$  vibrational modes are included in the amide groups. At  $1270\text{ cm}^{-1}$  ascribed to  $\text{NH}_2$  marker, which is very strong amide III mode for  $\alpha$ -sheet disorder conformation. Band at  $1268$ ,  $1286$ , and  $1296\text{ cm}^{-1}$  (amide III vibration of protein  $\alpha$ -helix structure) were identified in the SERS spectra of other viruses [17, 18].  $\text{CH}(\text{CH}_2)$  bending modes markers in proteins and nucleic acids are responsible for the next strong peak at  $1453\text{ cm}^{-1}$ . Amino acids and purines molecules are probably to promote adsorption on hot spot located on AgNPs' surface, allowing for an enhancement in the vibration of these molecules at  $1095\text{ cm}^{-1}$ , a medium-intense band can be assignable to the complex symmetrical mode of  $\text{PO}_2^-$  marker, which is composed of nucleic

acids (Fig. 6A). However, in the SERS spectrum of Fig.6B, this band appears to have shifted slightly to  $1075\text{ cm}^{-1}$ , a strong band at  $1070\text{ cm}^{-1}$  attributed to ( $\gamma$ -C-N) also identified in the SERS spectra of other viruses [17,18]. This spectral shift can be attributed to the molecular layers coating the AgNPs, and the relative intensity of the molecular components is modulated by the orientation of the adsorbate onto the AgNPs surfaces. The next medium-intense bands appear at  $1144\text{ cm}^{-1}$  which correspond to C-N stretching proteins marker, and at  $1500\text{ cm}^{-1}$ , which is due to the presence of amide II ( $\nu(\text{C}=\text{C})$ ) in benzenoid ring, indicating that SARS-CoV-2 molecules are adsorbed to AgNPs carboxyl groups and other molecules related to amino groups. The ring breathing modes in purine DNA/RNA are assigned to the low-broad intense at  $733$  (Fig. 6A) and  $743$  (Fig. 6B), probably from building blocks created during amino acid catabolism. A virion (also called a virus, or particle) is made up of DNA or RNA molecules surrounded by a protective coat of proteins [32]. Tyr, Trp, Adenine, Guanine (DNA/RNA); C=C bending mode of Phenylalanine markers, can also be ascribed to the next low-broad intensity at  $1580\text{ cm}^{-1}$  [33, 34]. Low intensity band at  $1405\text{ cm}^{-1}$  in the  $1300\text{-}1650\text{ cm}^{-1}$  region attributable to  $\text{CH}_2$  scissoring, shifted to  $1430\text{ cm}^{-1}$ , attributed to adenine or guanine, the band at  $1606\text{ cm}^{-1}$  from the phenyl ring bond-stretching vibrations, assigned to in-phase motion of  $\nu(\text{C}_8\text{-C}_e)$ . Low-intensity bands at  $1304$ ,  $1352$ , and  $1381\text{ cm}^{-1}$  (Fig. 6A) were ascribed to Amide III (protein) cytosine, purines (T,A,G), and tryptophan.. The next low intensity bands are seen at  $954$  and  $915\text{ cm}^{-1}$  which correspond to the proteins  $\nu(\text{C-O})$  and C-N and  $\nu(\text{C-COO}^-)$ . Interestingly, too weak bands (low intensities) at  $887$ ,  $834$ ,  $857$ , and  $781\text{ cm}^{-1}$  are due to phosphodiester, (O-P-O) stretching of thymine and RNA moieties in the deoxyribose molecule. Other low weak intensity bands at  $577$ ,  $612$ ,  $677$  and  $680\text{ cm}^{-1}$  were attributed C-C twisting mode of phenylalanine and adenine, purines. Furthermore, we discovered a peak at  $517\text{ cm}^{-1}$ , which is assigned to the protein's S-S stretching modes of cysteine residues in proteins, the band at  $612\text{ cm}^{-1}$  appears in the Raman spectra of proteins as Phe ring breathing vibration corresponding to a homothetic motion of the ring breathing atoms C-C twist. Finally, the remaining two bands the first at  $457\text{ cm}^{-1}$  assigned to amino acids with a cyclic R side, such as Phe or Trp, suggesting that the carboxyl groups ( $\text{r}(\text{COO}^-)$ ) are chemically adsorbed to AgNPs [19, 17]. The appearance of the band at  $2100\text{ cm}^{-1}$  in our samples is most likely due to dehydration of the peptide bond, which results in results in  $\nu(\text{C}\equiv\text{C})$  or  $\nu(\text{C}\equiv\text{N})$  due to degradation (peptide and protein residues) caused by laser power. The last band at  $2935\text{ cm}^{-1}$  can be assigned to asymmetric and symmetric  $\text{CH}_3$  stretching vibrations of the methyl end groups of membrane lipids as well as the methyl side groups in cellular proteins. These molecules are most likely derived from E and S SARS-CoV-2 proteins associated with glycoproteins, which includes a bilayer lipid envelope outside the protein coat. (Fig. 6B, and Table 1). Using highly SERS active aggregated AgNPs substrate to identify SARS-CoV-samples, adsorption of biomolecules including proteins, peptides of SARS-CoV-2 onto the surface of AgNPs depends on the chemical origin of the biomolecules and SERS enhanced mechanism, which entails changes in frequency and intensity that are primarily related to the distance between AgNPs colloids and groups of SARS-CoV-2 biomolecules.

**TABLE 1** Tentative SERS bands assignments of SARS-CoV-2 main Raman shift vibrational modes

Range (cm <sup>-1</sup> )		Tentative Assignments <sup>Ⓜ</sup>
500-1700	300-3500	
=	457	r(COO <sup>-</sup> ); Phe, Tyr
517	=	ν(S-S) disulfide (amino acid cysteine) <sup>Ⓜ</sup>
557	557	C-C twist mode of Phe (proteins)
612	612	C-C twist mode of Phe; δ(COO <sup>-</sup> )
677	680	Tyr
733	743	A,U, T, C, ring breathing modes in the DNA/RNA
781	=	ν(O-P-O) RNA
834	857	ν <sub>s</sub> (O-P-O) str, T
887	887	DNA/RNA, phosphodiester, deoxyribose
915	=	ν(C-COO <sup>-</sup> )
954	=	ν(C-O) and C-N of proteins
1007	1007	δ(C-C) aromatic ring in Phe
1095	1095	ν(C-N), ν(PO <sub>2</sub> <sup>-</sup> ) nucleic acid,
1144	1144	C-N stretching in proteins, t(NH <sub>2</sub> )
1221	1221	Amide III, ν as (PO <sub>2</sub> <sup>-</sup> ), δ(NH <sub>2</sub> )
1270	1270	Amide III, δ(NH <sub>2</sub> )
1304	1305	Amide I, C-H def
1352	1352	A,G C-H def
		ν <sub>s</sub> (COO <sup>-</sup> )
1381	1381	ρ(C-H)
1405	1405	CH <sub>2</sub> sciss, G,A
1453	1453	δ(CHCH <sub>2</sub> ), proteins and lipids
1500	1500	δ(C=C) in benzenoid ring, amide II
1580	1580	A,G (DNA/RNA), C=C bending mode of Phe
		ν <sub>s</sub> (COO <sup>-</sup> ), Tyr, Trp

1606	1606	Phe ring bond vibration, in-phase motion of $\nu(\text{C}_\delta\text{-C}_\epsilon)$
=	2100	$\nu(\text{C}\equiv\text{C})$ , $\nu(\text{C}\equiv\text{N})$ , peptides residues
=	2935	$\nu(\text{C-H})$ , $\nu(\text{C-H}_3)$ membrane of lipids

☒ All the assignments are from references [18, 27, 28, 29,30, 31]

☒  $\nu$ , stretching;  $\delta$ , bending;  $\rho$ , rocking;  $\tau$ , torsion; wagg, wagging; twist, twisting,; sciss, scissoring; def, deformation; as, asymmetric; s, symmetric; C, cytosine; T, thymine; Aadenine; G, guanine; U, uracil; Phe, phenylalanine; Tyr, tyrosine, Trp, tryptophan.

## 4. Conclusion

A novel, simple, quick, and accurate technology for acquiring strong, sharp, and reproducible SERS signal intensities was developed. When compared to normal Raman spectra, the SERS approach resulted in an intensity enhancement of over  $10^5$  fold. The SERS spectra obtained exhibited significant consistency, sensitivity and selectivity. We also studied the spectral reproducibility and virus detection limit of SARS-CoV-2 virus SERS spectra at different concentrations  $10^2$  and  $10^5$  vp/mL, and the LOD achieved lower than  $10^3$  vp/mL. RSDs of less than 20%. The major vibrational sharp and intense signal in the SERS spectrum of SARS-CoV-2 was found at 1007, 1221, 1270, and  $1453\text{ cm}^{-1}$  in the  $500\text{-}1700\text{ cm}^{-1}$  range, and 457 and  $2395\text{ cm}^{-1}$  in the  $300\text{-}3500\text{ cm}^{-1}$  region. Furthermore, these bands were ascribed to typical biomolecules found in the major structural proteins of SARS-CoV-2. The most prominent bands from nucleic acids were identified by the SERS spectra of the SARS-CoV-2 fingerprint: aromatic amino acid side chains:  $1007\text{ cm}^{-1}$  (Phe marker),  $1095\text{ cm}^{-1}$  (C-N and  $\text{PO}_2^-$  markers),  $1580\text{ cm}^{-1}$  (A, G, Tyr, Trp markers). Vibrations of the protein main chain:  $1144\text{ cm}^{-1}$  (C-N and  $\text{NH}_2$  markers),  $1221\text{ cm}^{-1}$  (CN and NH markers),  $1270\text{ cm}^{-1}$  ( $\text{NH}_2$  marker),  $1453\text{ cm}^{-1}$  ( $\text{CHCH}_2$  marker). Development of improved detection and characterization is primarily means of controlling SARS-CoV-2 virus infection spread everywhere, in order to battle COVID-19 infectious disease. Finally, the SERS technique we proposed for detecting, characterizing and monitoring of SARS-CoV-2 variants is quick, precise, and cost-effective, with high sensitivity.

## Declarations

### Ethical Approval and Consent to participate

Not applicable

### Consent for publication

Not applicable

## Availability of data and materials

Not applicable

## Competing interests

The authors declare that they have no competing interests.

## Funding

No specific funding was obtained for the preparation of the manuscript.

## Authors' contributions

J.C., Ramirez-Perez, wrote the proposal, planned the analytical methods, run the experiments, and wrote the manuscript. D. Durigon, acquired samples and revise the proposal and final manuscript. All authors participated in review language, read corrections and approved the final manuscript.

## Acknowledgements

The authors gratefully acknowledge the support of the Research Unity in Astrobiology NAP-Astrobio/IAG-University of Sao Paulo-Brazil for allowing us to use the Rainshaw Raman Equipment for this research.

## Authors' information

Javier C. Ramirez Perez, visiting Professor Institute of Physics, University of Sao Paulo, Brazil. ORCID: <https://orcid.org/0000-0001-9596-8281>

Danielle.Durigon, Department of Microbiology, Institute of Biomedical Sciences, ICB, University of Sao Paulo, Brazil.

## References

1. Ramadan, N., Shaib, H. "Middle east respiratory syndrome coronavirus (MERS-COV):A review" 2019. In GERMS, <https://doi.org/10.18683/germs.2019.1155>
2. Sohrabi, D., Alsafi, Z., O'Neill, N., Khan, M., Kerwan, A., Al-Jabir, A., Losifidis, C, Agha, R. "WHO declares global emergency:A review of the 2019 novel coronavirus (COVID-19)". In International Journal of Surgery, <https://doi.org/10.1016/j.ijsu.2020.02.034>
3. Wang, Y., Chen Y., Qin, Q. "Unique epidemiological and clinical features of the emerging 2019 novel coronavirus pneumonia (COVID-19) implicate special control measures". Journal of Medical Virology. <https://doi.org/10.1002/jmv.25748>
4. <https://www.who.int/docs/default-source/coronaviruse/situation-reports/20201020-weekly-epi-update-10.pdf>.

5. C-C. Lai, T-P. Shih, W-C. Ko, H-J.Tang, P-R Hsueh. "Severe acute respiratory syndrome coronavirus 2 (SARS-CoV-2) and coronavirus disease 2019 (COVIS-19):The epidemic and the challengues". 2020. *Int J Antimicrob Agents*, 55: 105924.
6. F. Xiao, M. Tang, X. Zheng, Y. Liu, H. Shan "" Evidence for gastrointenstinal infection of SARS-CoV-2". 2020. *Gastroenterology*, 158: 1831–1833.
7. D. Zhang, X. Zhang, R. Ma, S. Deng, X. Wang, X. Zhang, X. Huang, Y. Liu, G. Li, J. Qu, Y. Zhu, J. Li. "Ultra-fast and onsite interrogation of Severe Acute Respiratory Syndrome Coronavirus 2 (SARS-CoV-2) in environmental specimens via surface enhanced Raman scattering (SERS)". *medRxiv*. 2020. [hppt://doi.org/10.1101/2020.05.0220086876](https://doi.org/10.1101/2020.05.0220086876)
8. M.L. Holshue et al. "Novel coronavirus in the United States". *New England Journal of Medicine*. 2020. 382: 929–936,
9. Wang et al. "Clinical Characteristics of 138 Hospitalized patients with 2019 novel coronavirus-infected Pneumonia in Wuhan China". *JAMA*. 2019. 33:1061–1069.
10. S. Stöckel, J. Kirchhoff, U. Neugebauer, P. Rosch, and J. Popp." The Application of Raman spectroscopy for the detection and identification of microorganisms" *Review: J. of Raman Spectroscopy*. 2016. 47: 89–109.
11. S. Bahavya, RF., Renee, H-Anne-Isabelle, R. Emile, PVD., Richard. "SERS: material, applications, and the future." 2012, *Materials* 15,16 – 15.
12. J.C. Ramirez-Perez, T. Alves dos Reis, M. Rizzutto. "Identifying and detecting Entomopathogenic fungi using SERS 2021. *BAJER*, 4(4), 4832–4350. <https://doi.org/10.34188/bjaerv4n4-002>.
13. T.Zhong-Q, Y.Zhi-Lin, R.Bin, W.De-Yin. "SERS from transition metals and exited by ultraviolet light, in K. Katrin, K.Herald, M.Martin (Eds.), *Surface-enhanced Raman Scattering Physics and Applications*." Springer-Verlat Berlin Heidelberg, Germany 2006, 125–147.
14. M. Moscovits. "Surface-enhanced spectroscopy". 1985, *Rev.Mod. Phys.* 57, 783–826.
15. D. Shoeman D. and C.F. Burtram, "Coronavirus envelope protein; current knowledge" *Virology Journal*. 2019, 16:69, 1–22
16. Z.Ke, J.Oton, Qu K., M. Cortese, V. Zila, L McKeane, T Nkane, J.Zlvanov, C. Neufeldt, B.Cerlkan, R Bartenschlager, J.A.Briggs, " Structures and distribution of SARS-CoV-2 spike proteins o intact virions" *Nature*, article, 2020. <https://doi.org/10.1038/s41586-020-2665-2>
17. X. Y. Zhang, M.A., Young, O. Lyandres, R.P., Van Duyne. "Rapid detection of an anthrax biomarker by surface-enhanced Raman spectroscopy. *J.Am.Chem. Soc.* 2005.127 (12), 4484–4489.
18. C. Fan, Z. Hu, L.K Riley, G.A Purdy, A. Mustapha, M. Lin. "Detecting food-and waterborne viruses by surface-enhanced Raman spectroscopy." *Journal of Food Science*. 2010. 75 (5): 302–307.
19. P-Di Bao, T-Q. Huang, X-M, L., T-Q, W. "Surface-enhanced Raman spectroscopy of insect nuclear polyhedrosis virus" *J. Raman Spectrosc.*2001. 32:227–230.
20. F. Feldman, W. L. Shupert, E.Haddock, B. Twardoski, H. Feldmann."Gamma irradiatin as an effective method for inactivation on emerging viral pathogens". *Am.J.Trop.Med.Hyg.*2019, 100(5), 1275–

1277.

21. A. Leung, K. Tran, J. Audet, S. Lavineway, N. Bastien, J. Krishnan. "In vitro inactivation of SARS-CoV-2 using gamma radiation". *Applied Biosafety: Journal of ABSA International*. 2020, 1–4. <https://doi.org/10.1177/1535676020934242>.
22. P.C. Lee and D. Meisel, "Adsorption and surface-enhancement Raman of dyes on silver and gold sols" *J. Phys. Chem.* 1982. 86, 3391–3395.
23. K. Kneipp, Y. Wang, H. Kneipp, L.T. Perlman, I. Itzan, R.R. Dasari, M.S. Feld. "Approach to single-molecule detection using surface-enhanced resonance Raman-scattering (SERRS)-a study using Rhodamine 6G on colloidal silver." *Appl. Spectrosc.* 1997. 49:780–784.
24. Le Ru, E.C., Blackie, E., Meyer M., Etchegoin P.G. "Surface enhanced Raman scattering enhancement factors: A comprehensive study." *J. Phys. Chem.* 2007, 111, 13794–13803.
25. Wang, H-H., Liu, C.C., Wu, S.B., Liu N.W., Peng, C.Y. "Highly Raman enhancing substrates based on silver nanoparticle arrays with tunable sub-10 nm gaps." *Adv. Mater.* 2006. 18 (4), 491–495.
26. A. Rygula, K. Majzner, K.M. Marzec, A. Kaczor, M. Pilarczyk, M. Baranska. "Raman spectroscopy of proteins: a review." *Journal of Raman Spectroscopy*. 2013. 44: 1061–1076.
27. H. Wei, A. McCarty, J. Song, W. Zhou, P.J., Vikesland. "Quantitative SERS by hot spot normalization – surface enhanced Rayleigh band intensity as an alternative evaluation parameter for SERS substrate performance." *2017 Faraday Discuss*, 205, 491–504. <http://doi.org/10.1039/c7d00125h>
28. H. Deng and Q. He. "The study of Turnip Mosaic virus coat protein by surface enhanced Raman spectroscopy." *Spectrochimica Acta*. 1993. 49 (12): 1709–14.
29. S.A. Eichorst, F. Strasser, T. Woyke, A. Schintlmeister, M. Wagner, D. Wobken D. "Advancement in the application of NanoSIMS and Raman microspectroscopy to investigate the activity of microbial cells in soils." *FEMS Microbiology Ecology*. 2015. 91 (10): 1–14.
30. J.S. Ellis and M.C. Zamboni. "Molecular diagnosis of influenza." *Rev. Med. Virol.* 2002, 12, 375–389.
31. D. Newman. "FT-Infrared and FT-Raman Spectroscopy in biochemical research." *Appl. Spectrosc.* 2001. 36(2):239–98.
32. P. Hermann, A. Hermelink, V. Lausch, G. Holland, L. Möller, N. Bannert, and D. Naumann, "Evaluation of tip-enhanced Raman spectroscopy for characterizing different virus strains," *Analyst*. 2011, 136, 1148–1152.
33. P. Hermann, H. Fabian, D. Naumann, and A. Hermelink, "Comparative study of far-field and near-field Raman spectra from silicon-based samples and biological nanostructures," *J. Phys. Chem. C*. 2011, 115, 24512–24520.
34. T. Lemma, J. Wang, K. Arstila, V. P. Hytonen, J-J. Toppari. "Identifying yeasts using surface enhanced Raman spectroscopy" *Spectrochimica Acta Part A: Molecular and Biomolecular Spectroscopy*. 2019, 218, 299–307.
35. P. R.A.F., Garcirasmik, K. Pappert, W. Wlysses, L. Otubo, M. Epple, C.L.P., Olivera, "An in situ SAXS investigation of the formation of silver nanoparticles and bimetallic silver-gold nanoparticles in

controlled wet-chemical reduction synthesis." *Nanoscale Advances*.2020, 2 (1):225–238. doi: 10.1039/c9na00569b.

36. M.J., Baker, J. Trevisan, P. Bassan, R. Bhargava, HJ Butler, K.M., Dorling,... and F.L. Martin. "Using Fourier transform IR spectroscopy to analyze biological materials," *Nature Protocols* 2014, 9 (8), 1771–1778. [http://doi.org/ 10.1038/nprot.2014.110](http://doi.org/10.1038/nprot.2014.110)
37. M.J., Baker, J. Trevisan, P. Bassan, R. Bhargava, HJ Butler, K.M., Dorling,... and F.L. Martin. "Using Fourier transform IR spectroscopy to analyze biological materials," *Nature Protocols* 2014, 9 (8), 1771–1778.
38. Ramirez-Perez J.C., Alves, T., Olivera C., Rizzutto, M. "Impact of silver nanoparticles size on SERS detection and identification of filamentous fungi," *Spectrochimica acta Part A: Molecular and Biomolecular Spectroscopy* 2022, 272, 120980. <https://doi.org/10.1016/j.saa.2022.120980>

## Figures

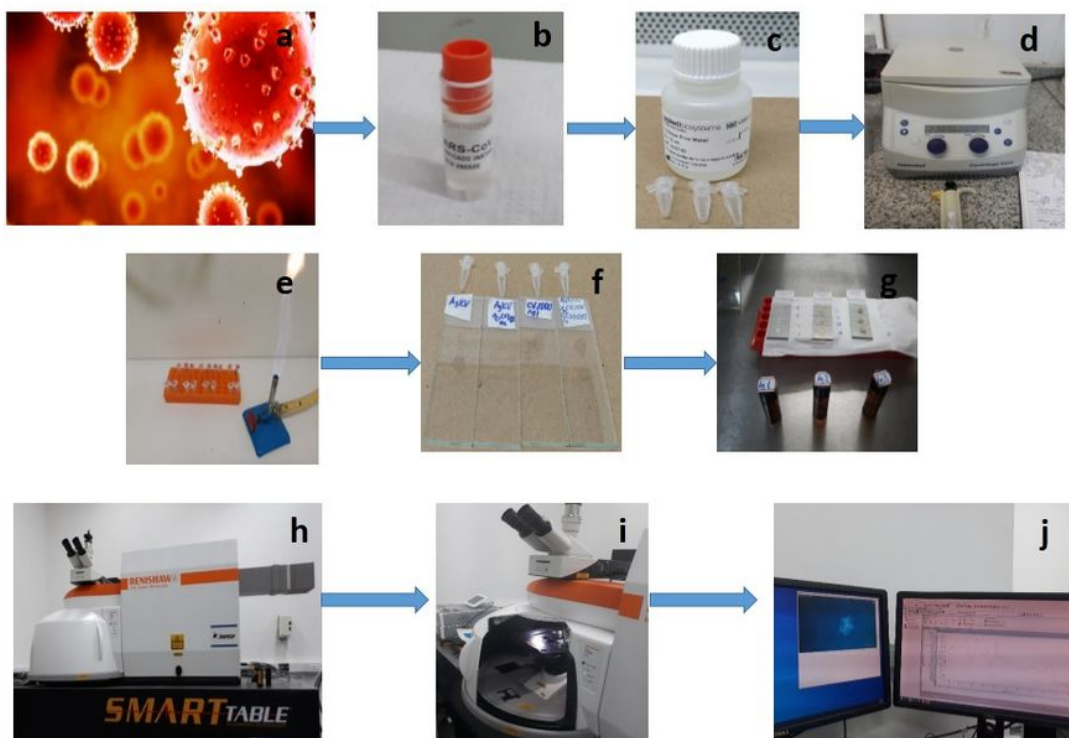


**Figure 1**

The experimental set up for the SERS tests is represented schematically in this diagram: (a) SARS-CoV-2 illustration; (b) Inactivated SARS-CoV-2 sample; (c) Water, nuclease-free molecular biology grade; (d) Centrifugation of sample; (e) SARS-CoV-2 sample preparation; (f) Control SARS-CoV-2 sample spiked on  $\text{CaF}_2$  glass slide; (g) SARS-CoV-2 mixed into AgNPs aggregates (SARS-CoV-2-AgNPs active substrate)

cast dried thin film; (h) Renishaw Raman system equipped microscopy and 785 diode laser source; (i) Microscopy sample stage; (j) SERS spectrum of SARS-CoV-2

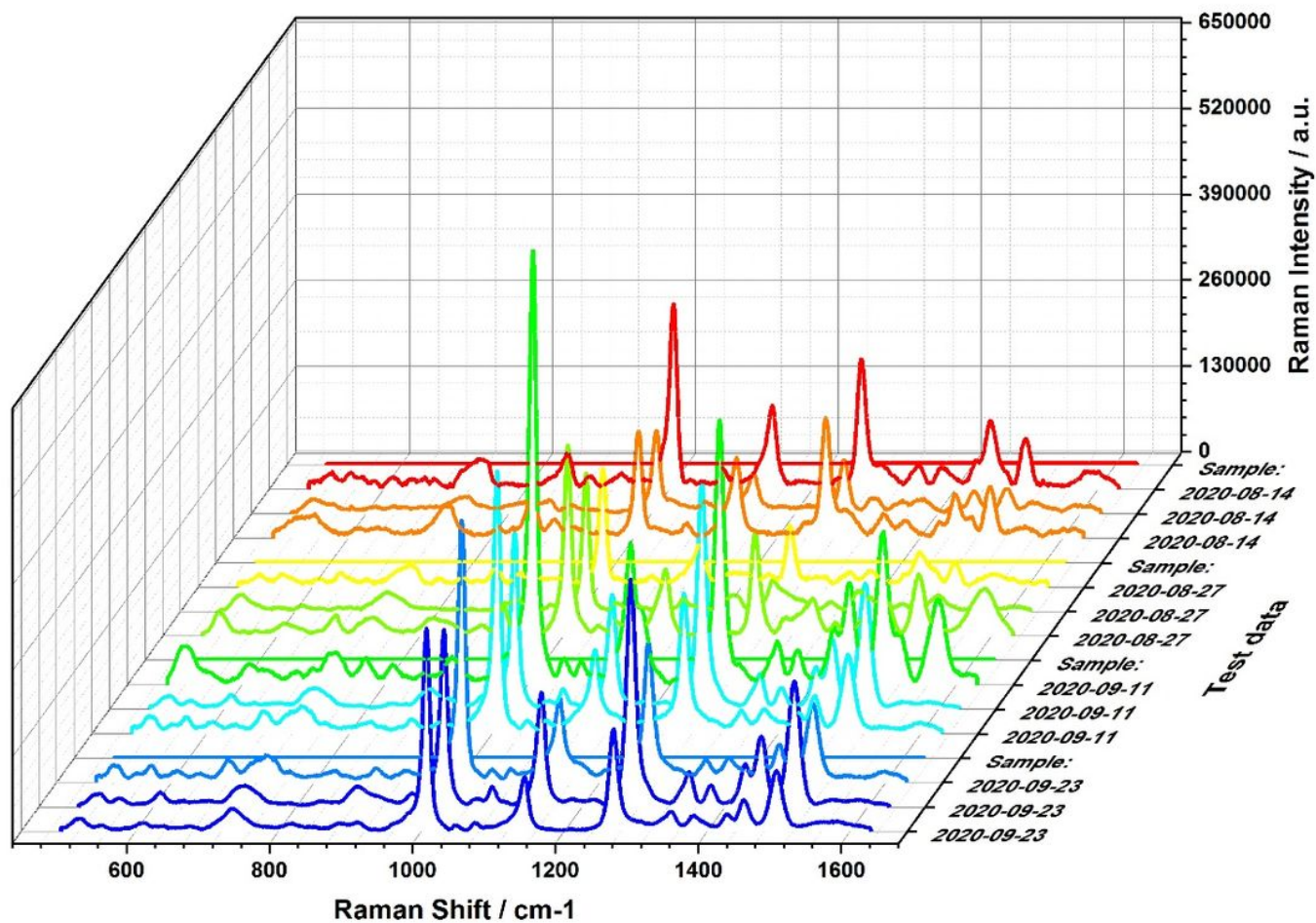


**Figure 2**

The representative of three-dimensional SERS spectra during the period of August 14 to September 23, 2020, the average SERS spectra of 12 samples of SARS-CoV-2 virus cells. SERS spectra were averaged from 18 different spots on a single sample for each spectrum.

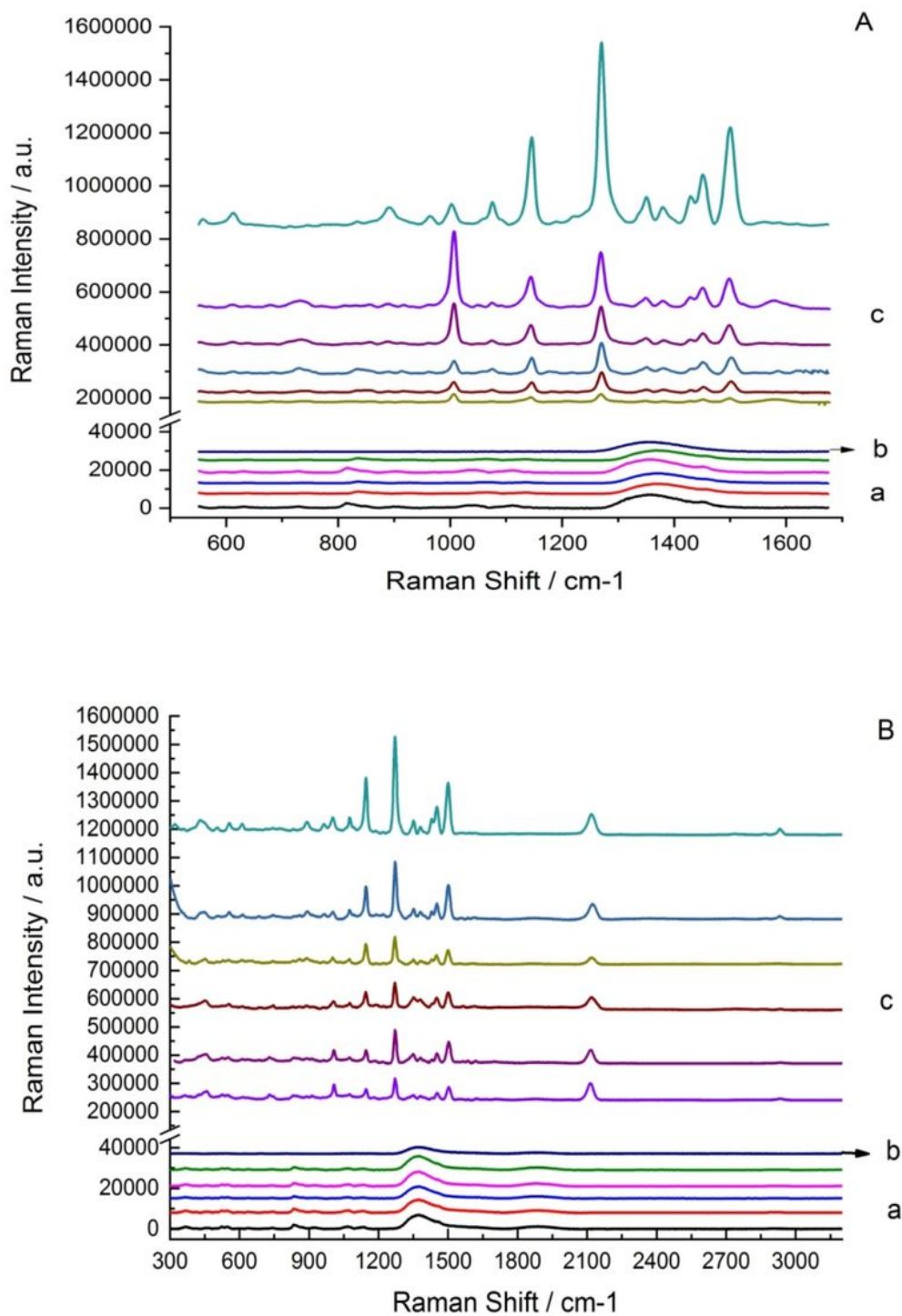


**Figure 3**

The representative Raman/SERS spectra in the regions A) 500-1700 cm<sup>-1</sup>; and B) 300-3500 cm<sup>-1</sup> region. are compared. Aa) and Ba) NR without AgNPs; Ab) and Bb) Clean Ca<sub>2</sub>F glass slide; Ac) and B-c) SARS-CoV-2- AgNPs-SERS substrate.

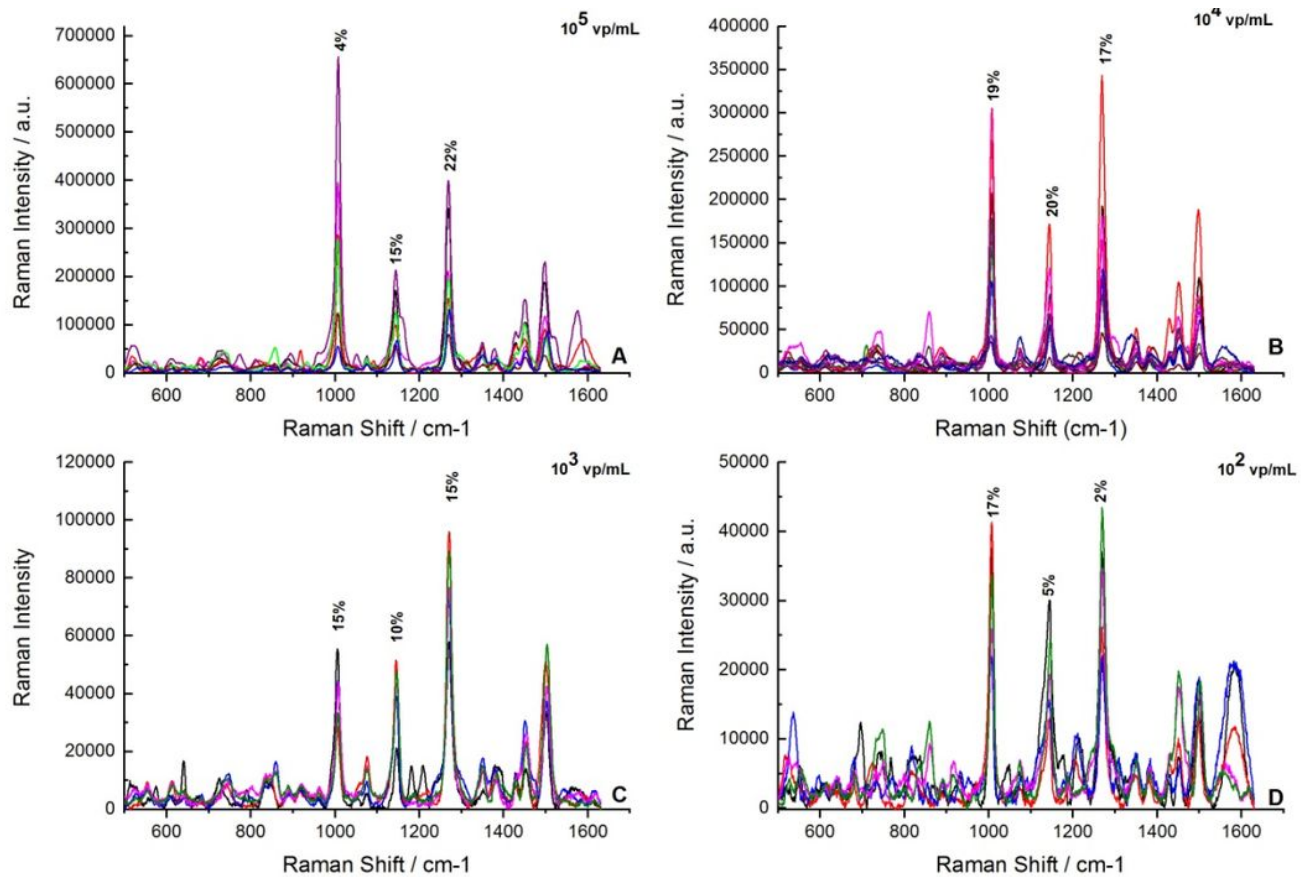


**Figure 4**

The SERS spectra of SARS-CoV-2 with various concentrations and Av.STD (%) of selected bands at: 1007, 1144 and 1270 cm<sup>-1</sup>: A)  $10^5$  vp/mL B)  $10^4$  vp/mL; C)  $10^3$  vp/mL; D)  $10^2$  vp/mL.

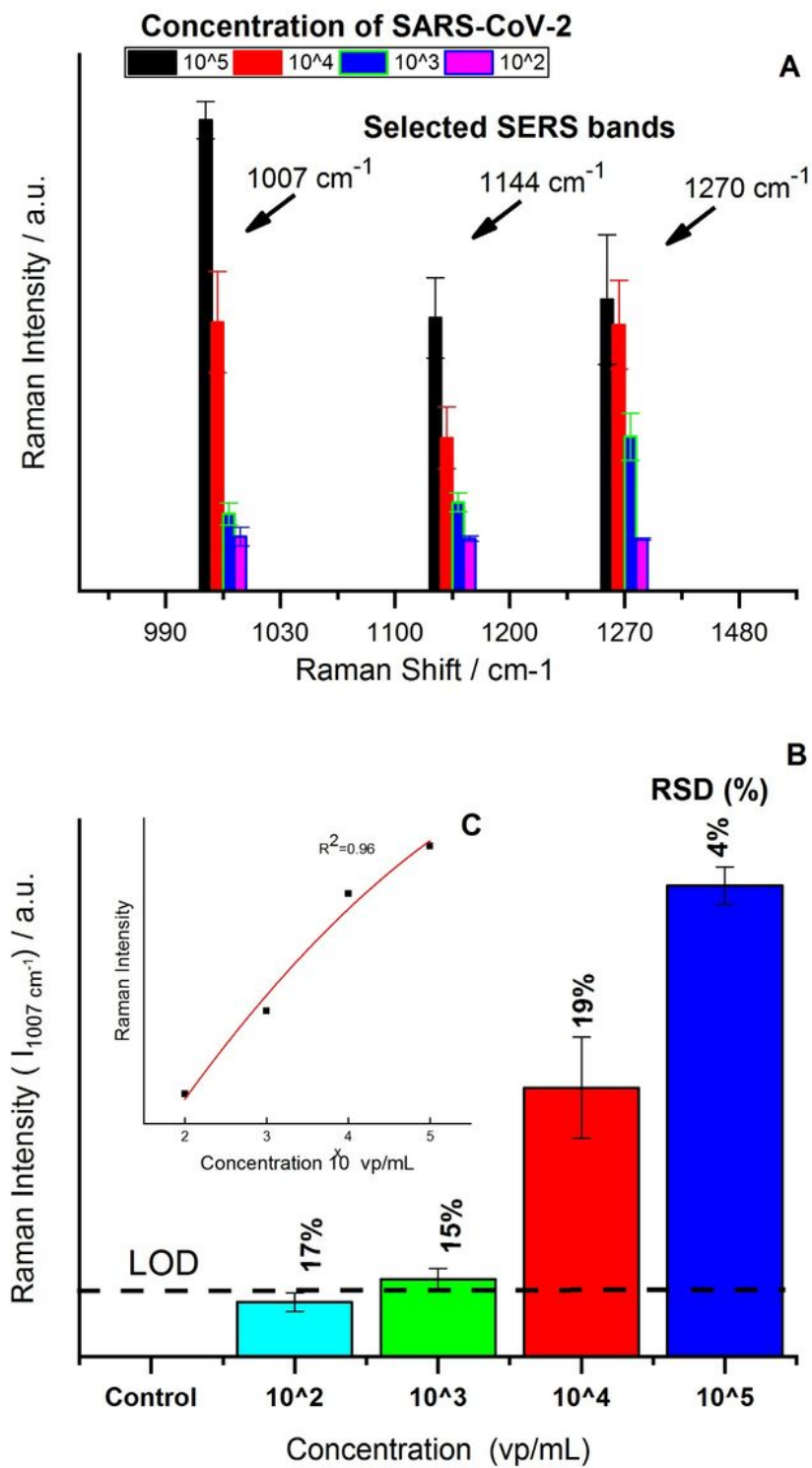


**Figure 5**

A) SERS band intensities at 1007, 1144, and 1270 cm<sup>-1</sup> as a function of SARS-CoV-2 concentration: 10<sup>5</sup>, 10<sup>4</sup>, 10<sup>3</sup> and 10<sup>2</sup> vp/mL. B) For LOD determination, the relative standard deviation (RSD %) for the selected band at 1007cm<sup>-1</sup> as a function of SARS-CoV-2 concentration. C) The inset shows the correlation of Raman intensity with concentration at 1007 cm<sup>-1</sup>.

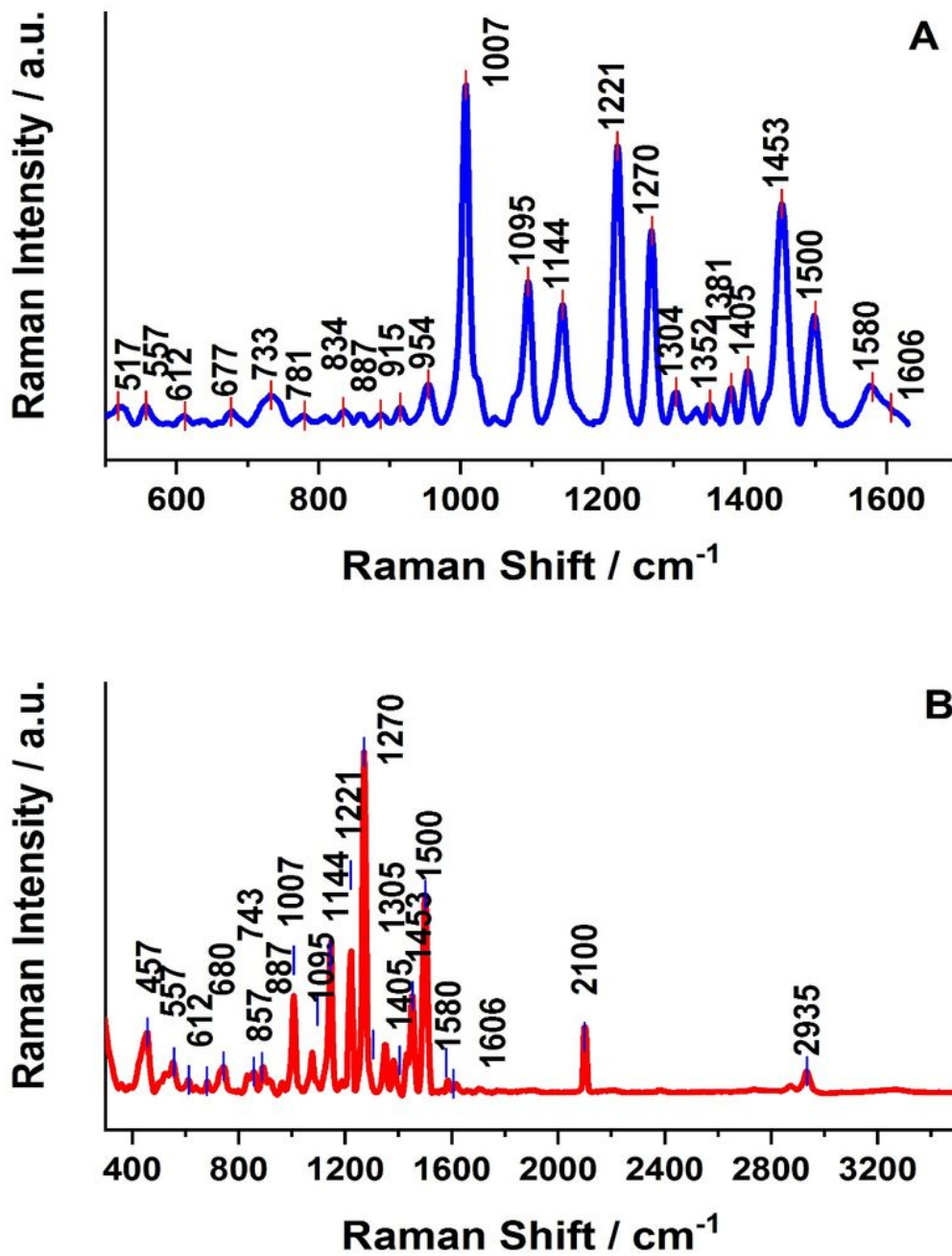


Figure 6

The average SERS spectra of SARS-CoV-2 using AgNPs deposited onto  $\text{CaF}_2$  glass slide platform cast dried thin film. Each SERS spectrum was obtained by averaging 18 measurements recorded at random location across the sample. The experimental conditions were: 1% (500 mW), 785 nm excitation, 10 s

exposure time. All SERS spectra were base line corrected and normalized and shifted vertically for improved visualization in the spectral range A) 500-1700  $\text{cm}^{-1}$ ; and B) 300-3500  $\text{cm}^{-1}$ .

## Supplementary Files

This is a list of supplementary files associated with this preprint. Click to download.

- [SupplementaryMaterialsSARSCoV2.docx](#)
- [floatimage1.jpeg](#)